A Second Quantization Model of Coupled Transmon Qubits

James Saslow, Kyle Nyguen
San Jose State University

Abstract

This project is a literature review and exploratory investigation of coupled transmon qubits. We show that the transmon can be sufficiently modeled by a quantum harmonic oscillator, since its skewed potential well allows energy states truncated to the computational basis, a requirement for qubits. Furthermore, we couple two flux-tunable transmon qubits, investigate its Hamiltonian in the second quantization, and understand the quantum dynamics of the system. Finally, we represent their dynamics in a spacetime-inspired description and show that by solving the two-body transmon problem, we effectively solve the n-body problem by considering the dynamics of all n transmons as a series of controlled, isolated two-body interactions.

1 The Quantum Harmonic Oscillator

A Review

1.1 Commutation Relations, Creation and Annihilation

The Hamiltonian of the Quantum Harmonic Oscillator (QHO) can be constructed as follows

$$\mathcal{H} = \frac{\hat{p}^2}{2m} + \frac{1}{2}m\omega^2\hat{x}^2 \tag{1}$$

where, in the first quantization, $\hat{x} = x$ and $\hat{p} = -i\hbar\frac{\partial}{\partial x}$.

And, the commutators between two operators, $\hat{A}$ and $\hat{B}$ is defined as

$$[\hat{A}, \hat{B}] \equiv \hat{A}\hat{B} - \hat{B}\hat{A} \tag{2}$$

We find that $\hat{x}$ and $\hat{p}$ do not commute[3]

$$[\hat{x}, \hat{p}] = i\hbar \tag{3}$$

The Raising and Lowering Operators are defined as

$$\begin{cases} \hat{a}^\dagger = \sqrt{\frac{m\omega}{2\hbar}}(\hat{x} - i\frac{\hat{p}}{m\omega}) & \text{(Raising)} \\ \hat{a} = \sqrt{\frac{m\omega}{2\hbar}}(\hat{x} + i\frac{\hat{p}}{2m}) & \text{(Lowering)} \end{cases} \tag{4}$$

The operators $\hat{a}^\dagger$ and $\hat{a}$ also have the property

$$[\hat{a}, \hat{a}^\dagger] = 1 \tag{5}$$

Using these raising and lowering operators, we rewrite the Hamiltonian in the second quantization:

$$\mathcal{H} = \hbar\omega\Big(\frac{1}{2} + \hat{a}^\dagger\hat{a}\Big) \tag{6}$$

1.2 The QHO Energy Spectrum

The reason we care about writing the Hamiltonian in the second quantization is because

of the impact the ladder operators have on shifting up and down energy levels.

Let's analyze this second quantized Hamiltonian in the context of the Time-Independent Schrodinger Equation (TIDSE)

$$\mathcal{H}\psi(x) = \varepsilon\psi(x) \tag{7}$$

Starting from an arbitrary state $\psi(x)$, we find that $\hat{a}\psi(x)$ *lowers* the energy of $\psi(x)$ by $\hbar\omega$

$$\mathcal{H}\Big(a\psi(x)\Big) = (\varepsilon - \hbar\omega)\Big(a\psi(x)\Big) \tag{8}$$

and $\hat{a}^\dagger\psi(x)$ *raises* the energy by $\hbar\omega$

$$\mathcal{H}\Big(\hat{a}^\dagger\psi(x)\Big) = (\varepsilon + \hbar\omega)\Big(\hat{a}^\dagger\psi(x)\Big) \tag{9}$$

Although we can raise and lower the energy with $\hat{a}^\dagger$ and $\hat{a}$ respectively, we cannot apply unlimited applications of $\hat{a}$ to $\psi(x)$, because we will eventually reach energies equal to or less than 0, which is non-physical[3]. This lower bound motivates the following boundary condition: $\hat{a}\psi_0(x) = 0$ where $\psi_0(x)$ is the ground state wavefunction. Given this boundary condition, we can derive ...

the ladder operator-eigenfunction relations,

$$\begin{cases} \hat{a}^\dagger\psi_n(x) = \sqrt{n+1}\psi_{n+1}(x) \\ \hat{a}\psi_n(x) = \sqrt{n}\psi_{n-1}(x) \end{cases} \tag{10}$$

the QHO energy spectrum,

$$\varepsilon_n = \hbar\omega\Big(n + \frac{1}{2}\Big);\ n \in \{0, 1, 2, ...\} \tag{11}$$

and finally, the QHO eigenfunctions[3]

$$\psi_n(x) = e^{-\frac{x^2}{2\alpha^2}} \frac{H_n(x/\alpha)}{\sqrt{\alpha 2^n n! \sqrt{\pi}}} \tag{12}$$

where $H_n(x)$ are the *Hermite Polynomials* and $\alpha \equiv \sqrt{\hbar/(m\omega)}$, the *characteristic length.*

2 The Quantum Anharmonic Oscillator

Qubits are Anharmonic

2.1 The Harmonic Oscillator is a Bad Qubit

The presence of equally spaced energy levels in the QHO implies leakage outside of the computational basis $|0\rangle$ and $|1\rangle$. For instance, say we have a harmonic oscillator in the $|1\rangle$ state. We could shoot a single photon's worth of energy $\hbar\omega$ at the oscillator, and it would either absorb the energy and transition to the $|2\rangle$ state, or perform spontaneous emission and decay to the $|0\rangle$ state. Either scenario could occur with equal probability, implying leakage. To contain our state within the computational basis, we must introduce anharmonicty into our potential well to generate unequally spaced energy levels.

2.2 The Duffing Oscillator

The Duffing Oscillator is an example of an anharmonic oscillator with anharmonicity α

$$\mathcal{H} = \hbar\omega\Big(\hat{a}^\dagger\hat{a} + \frac{1}{2}\Big) + \hbar\frac{\alpha}{2}\hat{a}^\dagger\hat{a}^\dagger\hat{a}\hat{a} \tag{13}$$

The anharmonicity is defined as

$$\alpha = \omega^{1\to2} - \omega^{0\to1} \tag{14}$$

If the energy levels are equally spaced, like in the QHO, then $\alpha = 0$. For the Transmon qubit, we will find that $\alpha < 0$ since the distance between energy levels decreases as we climb the ladder of energy eigenstates.

Treating the anharmonic term $V' \equiv \hbar\frac{\alpha}{2}a^\dagger a^\dagger aa$ as a small perturbation to the QHO energy spectrum[4], we can calculate an approximate energy spectrum for the first few energy levels of the duffing oscillator.

2.3 Anharmonic Energy Spectrum

Let ε_n be the energy spectrum of the anharmonic oscillator.

$$\begin{cases} \varepsilon_0 &= \frac{1}{2}\hbar\omega \\ \varepsilon_1 &= \frac{3}{2}\hbar\omega \\ \varepsilon_2 &= \frac{5}{2}\hbar\omega + \hbar\alpha \end{cases} \tag{15}$$

We observe that the energy levels of the anharmonic oscillator in the computational basis, i.e., the $|0\rangle$ and $|1\rangle$ states, do not change energy levels compared to their QHO counterpart. Although anharmonicity is essential for preventing qubit exploration into the $|2\rangle$ state and beyond, we can ignore anharmonic terms when doing analysis only on the computational basis.

2.4 The Transmon as an Anharmonic Oscillator

Let's do a real-life example of computing the anharmonicity α from a realistic Transmon energy spectrum.

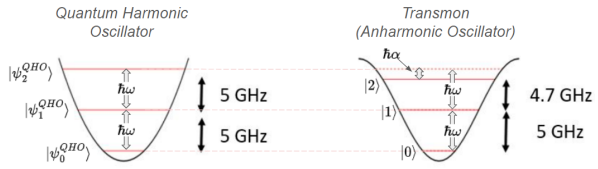

Figure 1: Comparing Energy Levels: The QHO and The Transmon. Adapted from[5]

where $|\psi_i^{QHO}\rangle$ is the ith eigenstate of the QHO and $|i\rangle$ is the ith eigenstate of the anharmonic oscillator.

In this exmaple, the qubit frequency is $\omega = 5$ GHz and the anharmonicity is

$$\begin{aligned} \alpha &= \omega^{1\to2} - \omega^{0\to1} \\ &= (4.7 \text{ GHz}) - (5 \text{ GHz}) \\ &= -300 \text{ MHz} \end{aligned}$$

Because a Transmon usually has a qubit frequency of $3-6$GHz and an anharmonicity magnitude of $100-300$MHz[1], this example is an accurate depiction of the Transmon quantized energy level landscape.

2.5 The Flux-Tunable Qubit

For a Transmon qubit to be physically realized as an anharmonic oscillator, it is constructed from a capacitor and a non-linear inductor called a Josephson Junction. A Josephson Junction is a superconducting element. If two Josephson Junction elements are wired in parallel, it forms a SQUID loop. Magnetic flux can be deposited into the SQUID loop to tune the qubit frequency ω. Such a qubit is called a *Flux-Tunable* Qubit. In the next section, we will explore how the variability of ω as a free parameter can aid in controlled entanglement schemes between two qubits.

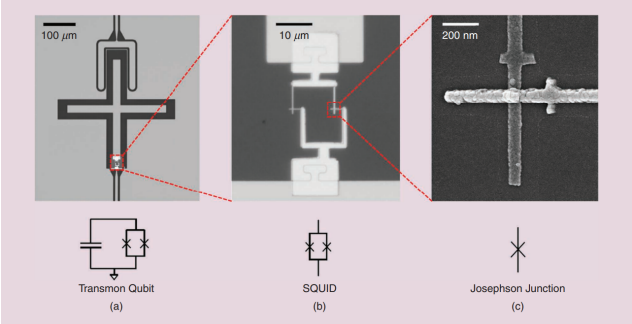

Figure 2: The Anatomy of a Flux Tunable Transmon Qubit. Adapted from[5]

3 Two Transmon Qubits

Quantum Circuit Electrodynamics and Entanglement

3.1 Coupled Transmons in the Second Quantization

Since we want to explore *electrical* harmonic oscillators, we must describe our oscillators in terms of *electrical* variables. In the electrical harmonic oscillator, the magnetic flux through the inductor $\hat{\Phi}$ and the charge on the capacitor plate $\hat{q}$ are the conjugate variables i.e. $[\hat{\Phi}, \hat{q}] = i\hbar$. This commutator relation suggests that the flux $\hat{\Phi}$ is the electrical analog of position $\hat{x}$, and that the charge is the electrical analog of momentum $\hat{p}$. In fact, in the electrical world, we can write our conjugate variables in terms of the typical ladder operators, which resemble what we found for $\hat{x}$ and $\hat{p}$, respectively[4].

$$\begin{cases} \hat{\Phi} &= \sqrt{\frac{\hbar}{2\omega C}}(a + a^\dagger) \\ \hat{q} &= -i\sqrt{\frac{\hbar\omega C}{2}}(a - a^\dagger) \end{cases} \tag{16}$$

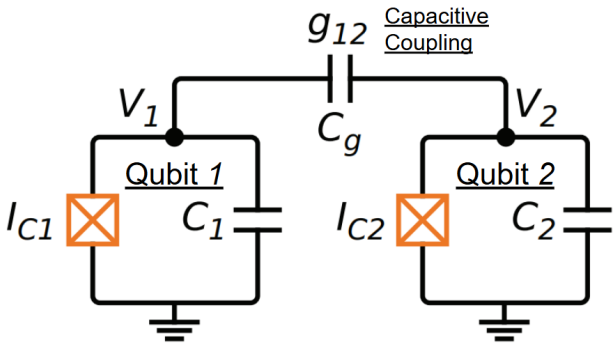

Figure 3: Directly capacitive coupling. Adapted from[1]

Both Qubit 1 and Qubit 2 are anharmonic oscillators given by a Hamiltonian composed of a harmonic and an anharmonic term:

$$\mathcal{H}_i = \hbar\omega_i\left(\hat{a}_i^\dagger\hat{a}_i + \frac{1}{2}\right) + \frac{\alpha_i}{2}\hat{a}_i^\dagger\hat{a}_i^\dagger\hat{a}_i\hat{a}_i$$

where $i \in \{1, 2\}$.

Classical circuit theory says that the interaction energy formed by weak capacitive coupling can be summarized as $\mathcal{H}_{int} = -C_g q_1 q_2$. If we upgrade the charge to a quantum operator i.e. $q_i \to \hat{q}_i$, and substitute in the charge operators written in terms of their corresponding ladder operators, we find

$$\mathcal{H}_{int} = -\hbar g(\hat{a}_1^\dagger - \hat{a}_1)(\hat{a}_2^\dagger - \hat{a}_2) \tag{17}$$

where $g = \frac{1}{2}\sqrt{\omega_1\omega_2}\frac{C_g}{\sqrt{C_g+C_1}\sqrt{C_g+C_2}}$ [1]

Therefore, the total Hamiltonian of the system described in the second quantization is

$$\mathcal{H} = \sum_{i\in\{1,2\}}\left[\hbar\omega_i\left(\hat{a}_i^\dagger\hat{a}_i + \frac{1}{2}\right) + \frac{\alpha_i}{2}\hat{a}_i^\dagger\hat{a}_i^\dagger\hat{a}_i\hat{a}_i\right] - \hbar g(\hat{a}_1^\dagger - \hat{a}_1)(\hat{a}_2^\dagger - \hat{a}_2)$$

3.2 The Hamiltonian as a Matrix

We found in section 2.3 that the computational basis states for harmonic and anharmonic oscillators are equivalent. Furthermore, due to the anharmonicty of the transmon qubit, we consider the domain of the energy spectrum to be truncated to the computational basis only. Therefore, we can omit the anharmonic term in the Hamiltonian and express the raising and lowering operators as raising and lowering matrices:

$$\hat{\sigma}^{\pm} \equiv \frac{\sigma_x \pm i\sigma_y}{2} \tag{18}$$

Applying the transformation:

$$\begin{cases} \hat{a}_i^{\dagger} & \to \hat{\sigma}_i^{+} \\ \hat{a}_i & \to \hat{\sigma}_i^{-} \end{cases} \tag{19}$$

we can recast the Hamiltonian in terms of Pauli-spin matrices (appendix A.1):

$$\mathcal{H} = \sum_{i\in\{1,2\}} \Big(-\frac{\hbar\omega_i}{2}\sigma_i^z \Big) + \hbar g \sigma_1^y \sigma_2^y \tag{20}$$

Performing the rotating frame approximation and dropping fast-oscillating terms[1], we derive a time-evolution unitary of the system in the rotating frame (denoted by the *tilde*) (appendix A.2)

$$\tilde{\mathcal{U}}_{qq} = \begin{pmatrix} 1 & 0 & 0 & 0 \\ 0 & f(t) & -iG(t) & 0 \\ 0 & -i[G(t)]^* & f(t) & 0 \\ 0 & 0 & 0 & 1 \end{pmatrix} \tag{21}$$

where

$$f(t) \equiv \cos\left(g\frac{\sin(\delta\omega\ t)}{\delta\omega} \right) \tag{22}$$

$$G(t) \equiv e^{-i\delta\omega}\sin\left(g\frac{\sin(\delta\omega\ t)}{\delta\omega} \right) \tag{23}$$

$$\delta\omega = (\omega_1 - \omega_2)/2 \tag{24}$$

In the limit where the detuning $\delta\omega$ is large, we see that the unitary approaches an identity gate $\tilde{\mathcal{U}}_{qq} \to \mathbb{I}^{\otimes 2}$, which makes intuitive sense since qubits largely separated in frequency should not interact

On the contrary, in the limit where we have perfect frequency matching between qubit 1 and 2 i.e. $\delta\omega = 0$,

$$\tilde{\mathcal{U}}_{qq} = \begin{pmatrix} 1 & 0 & 0 & 0 \\ 0 & \cos(gt) & -i\sin(gt) & 0 \\ 0 & -i\sin(gt) & \cos(gt) & 0 \\ 0 & 0 & 0 & 1 \end{pmatrix} \tag{25}$$

And, if we set the coupling to be $t = \frac{\pi}{2g}$ exactly, we derive the iSWAP gate:

$$\tilde{\mathcal{U}}_{qq}\left(t = \frac{\pi}{2g}\right) = \begin{pmatrix} 1 & 0 & 0 & 0 \\ 0 & 0 & -i & 0 \\ 0 & -i & 0 & 0 \\ 0 & 0 & 0 & 1 \end{pmatrix} \equiv \text{iSWAP} \tag{26}$$

The iSWAP gate is the native entanglement gate in the gate set for superconducting quantum computers. This entanglement gate, along with superposition gates, makes quantum computers fundamentally different from classical computers.

Interestingly, halving the coupling time results in a $\sqrt{\text{iSWAP}}$ gate which can be used to generate Bell-like maximally entanglement states[1]

$$\tilde{\mathcal{U}}_{qq}(t = \frac{\pi}{4g}) = \begin{pmatrix} 1 & 0 & 0 & 0 \\ 0 & 1/\sqrt{2} & -i/\sqrt{2} & 0 \\ 0 & -i/\sqrt{2} & 1/\sqrt{2} & 0 \\ 0 & 0 & 0 & 1 \end{pmatrix} \equiv \sqrt{\text{iSWAP}}$$

According to Google Quantum AI's documentation[2], their *Sycamore* 54-qubit device has a $\sqrt{\text{iSWAP}}$ gate execution time of 32 ns. Using this execution time, we can estimate the value of g for a real quantum computer to be $g \approx 24.5$ MHz. Since the qubit frequency is typically on the low GHz range, g is small compared to ω. Simple estimation reveals that $g/\omega \approx 0.1\%$.

3.3 Spacetime -Inspired visualization of Transmon Entanglement

Although we define these quantum circuit interactions in a mathematically abstract *Hilbert* Space, these transmon qubits exist in a physical location on the superconducting quantum chip and each have a world-line in spacetime[6].

Consider two qubits with large $\delta\omega$ such that they are decoupled and separated in frequency space. Qubit 1 is initialized in the $|0\rangle$ state and Qubit 2 is initialized in the $|1\rangle$ state, resulting in a total initial wavefunction of $|\psi_i\rangle = |0\rangle \otimes |1\rangle = |01\rangle$. Next, we apply flux-tuning to qubit 2 to lower its qubit frequency ω_2 to approach that of ω_1. Then, we let the 2 qubits interact for $\approx \frac{\pi}{4g}$ time to do a $\sqrt{\text{iSWAP}}$ gate. After that, we decouple the qubits by applying flux-tuning again to qubit 2 to create large detuning $\delta\omega$. The final state of the system should be a $\sqrt{\text{iSWAP}}$ applied to $|01\rangle$, which yields a bell-like state: $|\psi_f\rangle = \frac{1}{\sqrt{2}}\Big(|01\rangle - i\,|10\rangle\Big)$. Notice how each of these steps in generating a Bell State are described with frequencies ω_1 and ω_2 at some time t. Therefore, we can generate some spacetime-analog plot, (which we could call *frequency-time*, where ω is the spacetime analog of x) to model these interactions outside Hilbert Space.

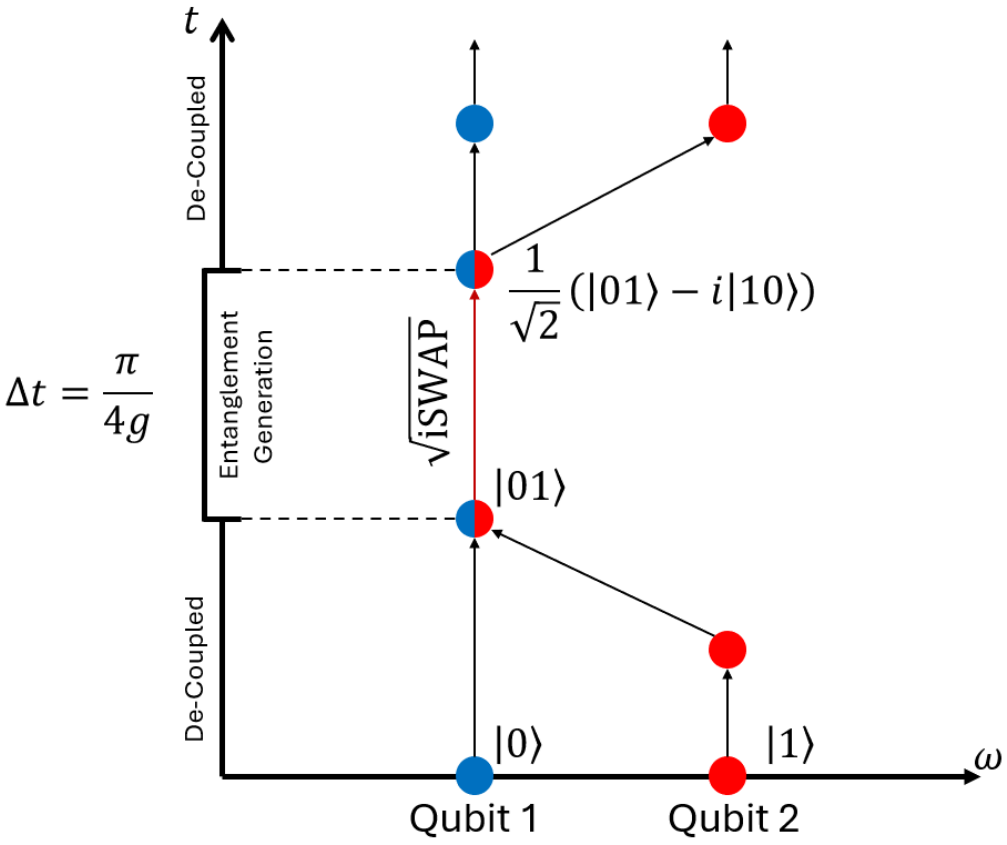

Figure 4: A "Frequency-time" description of two-qubit entanglement

Two-qubit $\sqrt{\text{iSWAP}}$ entanglement generation can be represented as a *frequency-time* plot. Where each arrow is the direction of time of evolution of each qubit. Two qubits only interact with one another when the worldlines of each qubit are intersecting, or very close to one another in frequency space. Due to the modularity of gate-based quantum computing, it turns out that the solution of the two-transmon problem can be generalized to solve

the n-transmon problem as long as we consider isolated two-body interactions for pairs of qubits. If we were to consider three-qubit world lines intersecting, we would end up with a three-body problem, which can be unstable. Therefore, treating an n-qubit system as an orchestrated sequence of isolated two-body interactions is a much safer alternative for multi-qubit control.

Let's consider what a *frequency-time* plot for three qubits might look like, considering this isolated two-body approach:

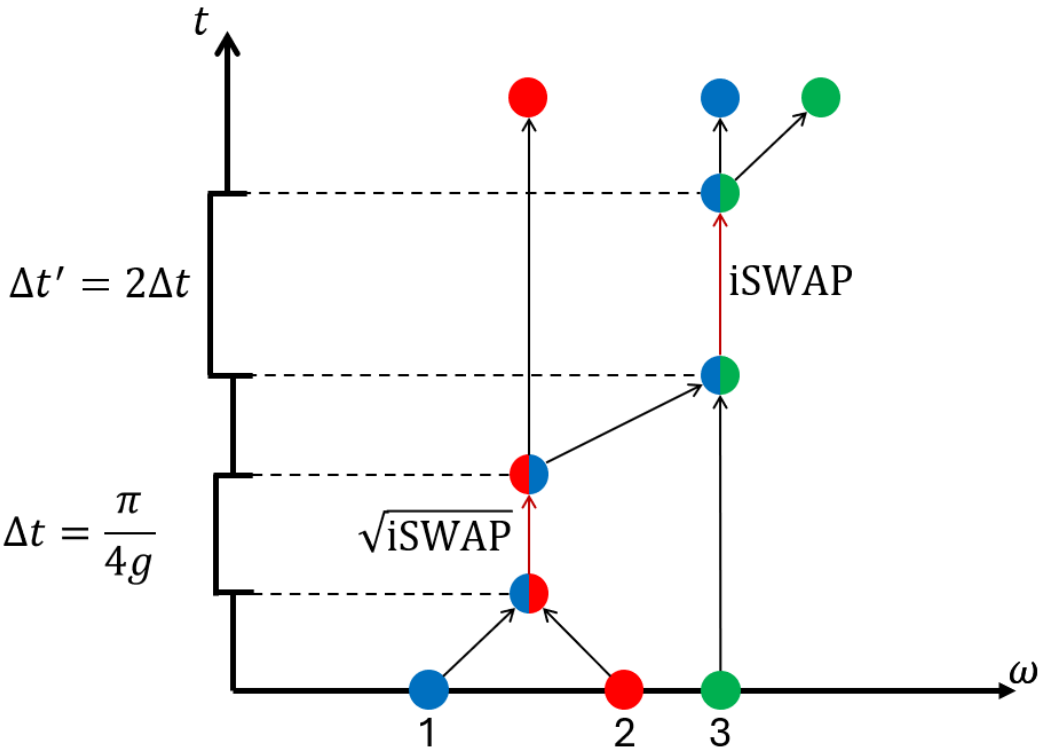

Figure 5: A "Frequency-time" description of three-qubit entanglement considering a modular connection of qubits

In a conventional quantum circuit diagram, this series of events may be represented as:

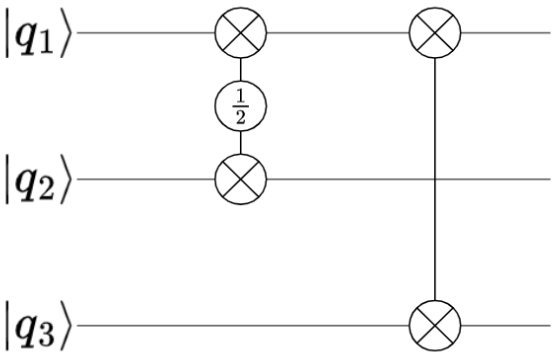

Figure 6: Three-Qubit Quantum Circuit

where the left-most operation is a $\sqrt{\text{iSWAP}}$ gate and the right-most operation is an iSWAP gate.

In this example, the three-qubit layout is modular such that each qubit has direct coupling with one another. In the case where there are a large number of transmon qubits and direct couplings are limited, a series of SWAP gates must be applied to transfer information of a physically distant qubit to a directly coupled one. This process is tedious, and often a bottleneck of performance in superconducting quantum computers.

4 Conclusions

In this investigative study, we performed a ground-up derivation of the transmon qubit starting with the quantum harmonic oscillator. We added anharmonicity to truncate the energy levels to the computational basis, a strict requirement for a qubit. After that, we explored the flux-tunable property of the transmon: The ability to adjust a Transmon's qubit frequency using an external magnetic field. Then, we coupled these qubits together and represented their interactions in a "spacetime"-like description. We found that once one solves the two-body problem for the coupled transmons, the n-body problem is complementarily solved. This extraordinary result reveals that a chaotic, n-body problem can be substituted for a series of controlled two-body interactions, physically realized through an orchestrated progression of isolated, fractional iSWAP gates.

References

[1] P. Krantz et al. A quantum engineer's guide to superconducting qubits. *Applied Physics Reviews*, 6(2):2–11, 2019.

[2] Google Quantum AI. Google devices : Cirq : google quantum ai. https://quantumai.google/cirq/google/devices#:~:text=duration%20of%2012ns.-,Square%20root%20of%20iSWAP,%2D0.5%20)%20is%20also%20available.&text=This%20gate%20has%20a%20duration%20of%2032ns.,been%20observed%20on%20some%20devices. Accessed: 2024-12-10.

[3] R. Shankar. *Principles of Quantum Mechanics*. Springer, New York, N.Y., 2nd edition, 2014.

[4] D. D. Stancil and G. T. Byrd. *Principles of Superconducting Quantum Computers*. John Wiley & Sons, Inc, Hoboken, NJ, 2022.

[5] R. Ma T. E. Roth and W. C. Chew. The transmon qubit for electromagnetics engineers: An introduction. *IEEE Antennas and Propagation Magazine*, 65(2):11–12, 2023.

[6] K. Wharton, R. Sutherland, T. Amza, R. Liu, and J. Saslow. A localized reality appears to underpin quantum circuits, Dec. 2024. Available at https://arxiv.org/abs/2412.05456.

5 Appendix

A Coupled Transmon Proofs

A.1 Recasting the 2nd Quantization of the Hamiltonian for Two Coupled Transmons in Terms of Pauli Operators

For a qubit (two-level system), we can omit the anharmonic term since we are focused on the first two energy levels. Also, the computational basis for the harmonic and anharmonic oscillators are equivalent. Therefore, we have

$$\mathcal{H} = \sum_{i\in\{1,2\}} \left[\hbar\omega_i \hat{a}^\dagger \hat{a}_i + \frac{1}{2}\right] - \hbar g(\hat{a}_1^\dagger - \hat{a}_1)(\hat{a}_2^\dagger - \hat{a}_2)$$

Because this is a two-level system, we can write the raising and lowering operators as raising and lowering matrices.

Multiplying raising and lowering matrices reveals that

$$\begin{cases} \sigma_i^+\sigma_i^- = \frac{\mathbb{I}-\sigma_i^z}{2} \\ (\sigma_1^+ - \sigma_1^-)(\sigma_2^+ - \sigma_2^-) = -\sigma_1^y\sigma_2^y \end{cases}$$

Making the substitution $\hat{a}_i^\dagger \to \sigma_i^+$ and $\hat{a}_i \to \sigma_i^-$ into our Hamiltonian while omitting constants since they have no impact on the spacing between energy levels, we derive

$$\mathcal{H} = \sum_{i\in\{1,2\}} \Big(-\frac{\hbar\omega_i}{2}\sigma_i^z\Big) + \hbar g\sigma_1^y\sigma_2^y \quad \square$$

A.2 Deriving the Time Evolution Unitary of Two Interacting Transmon Qubits

Defining $\mathcal{H}_0 \equiv \sum_{i\in\{1,2\}} \Big(-\frac{\hbar\omega_i}{2}\sigma_i^z\Big)$ to be the "Qubit" Hamiltonian and $\mathcal{H}_{qq} \equiv \hbar g\sigma_1^y\sigma_2^y$ to be the interacting Hamiltonian, we can analyze each component of the Hamiltonian separately as part of the Rotating Wave Approximation (RWA).

First, starting with the qubit Hamiltonian, we find its matrix form to be diagonal i.e. $\text{diag}[\mathcal{H}_0] = (-\hbar\bar{\omega}, -\hbar\delta\omega, +\hbar\delta\omega, +\hbar\bar{\omega})$, where $\delta\omega \equiv (\omega_1 - \omega_2)/2$ and $\bar{\omega} \equiv (\omega_1 + \omega_2)/2$. We find the qubit unitary evolution operator via a matrix exponential $\mathcal{U}_0 = \exp[-\frac{i}{\hbar}\int_0^t \mathcal{H}_0(t')dt']$. Because the qubit Hamiltonian is constant and diagonal,

$$\text{diag}[\mathcal{U}_0] = (e^{i\bar{\omega}t}, e^{i\delta\omega t}, e^{-i\delta\omega t}, e^{-i\bar{\omega}t})$$

We define the rotating frame unitary to be $\mathcal{U}_{RF} = \mathcal{U}_0^\dagger$, since the Hermitian conjugate of the qubit unitary cancels out the rotations caused by the qubit frequencies. Therefore, the qubit Hamiltonian in the rotating frame is $\tilde{\mathcal{H}}_0 = 0$. The interaction Hamiltonian in the rotating frame is given by $\tilde{\mathcal{H}}_{qq} = \mathcal{U}_{RF}\mathcal{H}_{qq}\mathcal{U}_{RF}^\dagger$ where the corresponding unitary transformation is $\tilde{\mathcal{U}}_{qq} = \exp[-\frac{i}{\hbar}\int_0^t \tilde{H}_{qq}(t')dt']$. Performing the matrix multiplication, and setting the fast oscillating terms to 0 as part of the RWA, we find

$$\tilde{\mathcal{H}}_{qq} \approx \hbar g \begin{pmatrix} 0 & 0 & 0 & 0 \\ 0 & 0 & e^{-2i\delta\omega t} & 0 \\ 0 & e^{2i\delta\omega t} & 0 & 0 \\ 0 & 0 & 0 & 0 \end{pmatrix}$$

Next, we perform the integral and matrix exponentiation to obtain the unitary in the rotating frame:

$$\tilde{\mathcal{U}}_{qq} = \begin{pmatrix} 1 & 0 & 0 & 0 \\ 0 & f(t) & -iG(t) & 0 \\ 0 & -i[G(t)]^* & f(t) & 0 \\ 0 & 0 & 0 & 1 \end{pmatrix} \quad \square$$

where

$$f(t) \equiv \cos\left(g\frac{\sin(\delta\omega\ t)}{\delta\omega}\right)$$
$$G(t) \equiv e^{-i\delta\omega}\sin\left(g\frac{\sin(\delta\omega\ t)}{\delta\omega}\right)$$
$$\delta\omega = (\omega_1 - \omega_2)/2$$